The searches for neutrinoless double beta decay and other physics with EXO-200

Yung-Ruey Yen
(on behalf of the EXO-200 and nEXO collaborations)
Department of Physics, Drexel Univeristy, Philadelphia, PA, U.S.A.

EXO-200 is a single phase liquid xenon detector designed to search for the neutrinoless double-beta decay of ^{136}Xe. The experiment uses enriched liquid xenon (110 kg in the active volume) in an ultralow background time projection chamber installed at the Waste Isolation Pilot Plant (WIPP), a salt mine with a 1600 m water equivalent overburden near Carlsbad, NM, USA. The detector has demonstrated excellent energy resolution and background rejection capabilities to set a limit of 1.1×10^{25}yr at 90% C.L. The physics results based on a 100 kg·yr exposure of ^{136}Xe are summarized. Recently, the experiment has restarted data taking after a two year hiatus due to unforseen WIPP incidents. The current electronic upgrades of EXO-200 and its restarted operation will help with the planning of tonne-scale next generation experiment, nEXO.

1 Introduction

Nuclear double-beta ($\beta\beta$) decay with the emission of two antineutrinos, first considered by Goeppert-Mayer in 1935 [1], is a second-order weak transition observed in a number of even-even nuclei. The two-neutrino decay mode ($2\nu\beta\beta$) to the ground state was directly observed in nine nuclei with half-lives in excess of 10^{18} yr, with ^{136}Xe being the longest at 2.2×10^{21} yr [2,3]. Decays with half-lives up to 10^{24} yr have been observed using indirect radiochemical and geochemical methods [4].

What is more interesting for the general neutrino community, at large, is the double-beta decay mode where zero antineutrino is emitted. Neutrinoless double beta decay ($0\nu\beta\beta$) represents physics beyond the Standard Model. In addition to the lepton number violation when the two electrons are produced without the two antineutrinos, the observation of $0\nu\beta\beta$ indicates that neutrinos are Majorana in nature - that a neutrino can turn into its own antiparticle. Neutrinos, the only fermions to be massive and electrically neutral, are the only known candidate to be a Majorana particle. In Figure 1, the Feynman diagrams for $2\nu\beta\beta$ (left) and $0\nu\beta\beta$ (right) are shown.

An observation of $0\nu\beta\beta$ can shed plenty of light on the nature of the neutrino. Most importantly, the measurement (or even just setting the limit) of $0\nu\beta\beta$ half-life ($T^{0\nu}_{1/2}$) can reveal information on the absolute mass of the neutrinos. The $0\nu\beta\beta$ half-life is directly related to

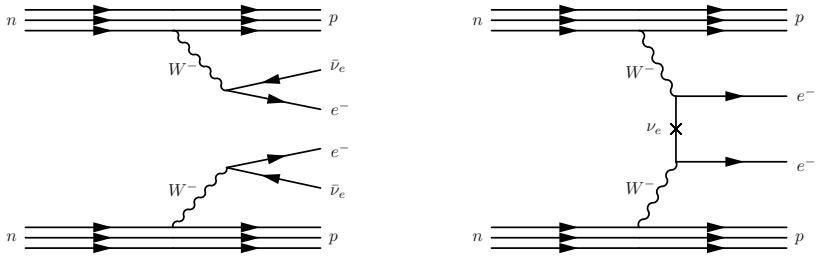

Figure 1 – The Feynman diagrams for $2\nu\beta\beta$ (left) and $0\nu\beta\beta$ (right).

the effective Majorana neutrino mass ($\langle m_\nu \rangle$) by a phase space factor (PSF, $G^{0\nu}(E_0, Z)$) and a nuclear matrix element (NME, $M^{0\nu}$) via the equation:

$$[T^{0\nu}_{1/2}]^{-1} = G^{0\nu}(E_0, Z) \left| M^{0\nu} \right|^2 \langle m_\nu \rangle^2, \tag{1}$$

where E_0 is the Q value and Z is the atomic number of the daughter nucleus. A sufficient sensitive $0\nu\beta\beta$ experiment can determine whether the various neutrino mass states are in the normal or the inverted hierarchies. Neutrino oscillation experiments can only measure the square of the mass-state differences; the ordering of the three known mass-states can result in either a higher total effective Majorana neutrino mass (inverted hierarchy) or not (normal hierarchy).

Alternatively, there may exist a new particle called a Majoron that can be created in a $0\nu\beta\beta$ decay. The Majoron, originally conceived as a Goldstone boson associated with the spontaneous lepton number symmetry breaking, can theoretically have different detailed characteristics. These various modes (spectral index) of the Majorons will result in different shapes of the observable sum electron spectrum, shown in Figure 2 left.

Back to the Standard Model, $2\nu\beta\beta$ decays to the first 0^+ excited state (0^+_1) of the daughter nucleus is an allowable process if this state is energetically accessible. Such is the case for ^{136}Ba as indicated in Figure 2 right. These decays are suppressed relative to their ground-state counterparts but are generally accompanied by the emission of de-excitation γs, creating a signature that is distinct from typical γ backgrounds and $2\nu\beta\beta$ decays to the ground state. The de-excitation is much too fast (few ps) to be temporally resolved by most practical detectors. Measurement of this decay can lead to better understanding of the fundamental nuclear physics, which may greatly decrease the uncertainty in the nuclear matrix element that goes into the Majorana effective mass calculations.

2 EXO-200

The searches for $0\nu\beta\beta$ decays boil down to measuring the two electron sum spectra in a very careful manner. In an ultra low background experiment with little radioactive impurities, $0\nu\beta\beta$ will manifest as a peak corresponding to the Q-value since all of the energies will go to the two β's in the absence of the neutrinos. A very good energy resolution is necessary to distinguish between the tail of the $2\nu\beta\beta$ spectrum and the $0\nu\beta\beta$ window (since the line will be smeared by realistic energy resolution of the detector).

The EXO-200 experiment is a single phase, liquid xenon time projection chamber (TPC) that uses 175 kg of xenon enriched to 80.6% in the isotope of ^{136}Xe, which has a relatively high Q-value of 2458 keV to be above most of the typical gamma backgrounds. The xenon can be purified with a zirconium getter [6] in situ while the experiment is running to minimize the amount of electronegative impurities. The xenon purity is further checked via the cold trap/mass spectrum method [7] to ensure impurities at only parts per billion level. Energy depositions in the liquid

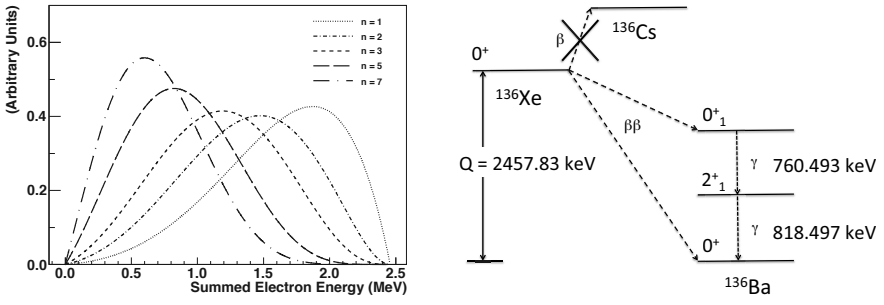

Figure 2 – The sum electron spectra for the various potential Majoron decays (left) and the energy level for ^{136}Ba excited states (right). Data for the energy level came from NNDC [5].

xenon creates both ionization and scintillation (at 178 nm), which are anticorrelated. EXO-200 measures both the ionization and the scintillation signals and exploits the anticorrelation between the two to achieve a good energy resolution.

The detector consists of two back-to-back cylindrical TPC's with a shared cathode at the center. Each TPC is 20 cm in radius and 22 cm in length with the anode consisting of two separate wire grids that are tilted by 60◦ from each other. For the ionization signals which creates electrons in the liquid xenon, the first grid measures an induction signal while the second grid measures the collection signal. Both grids consist of wires effectively separated by 9 mm. Behind the grids are an array of Large Area Avalanche Photodiodes (APDs) to measure the scintillation light. Teflon reflectors along the outside of the cylinder will reflect the UV scintillation light. The two wire grids allow for reconstruction of the charge deposit position in the plane perpendicular to the length of the cylinder (Z). The Z coordinate can be determined by the timing difference between the prompt scintillation signal and the ionization signal that depends on how far the electrons have to drift in the fixed electric field. More details can be found in EXO-200 detector paper [8].

To be shielded from cosmic ray, the EXO-200 detector is located at the Waste Isolation Pilot Plant (WIPP) near Carlsbad, NM, USA. The WIPP site has an overburden of 1585 meters water equivalent and is a salt mine, which has less natural Uranium and Thorium background than a hard rock mine. The detector is housed inside a clean room in the salt with the additional shielding of 25 cm of lead, 50 cm of a cryofluid known as HFE-7000, and about 5 cm of copper on all sides. Muon veto panels on 6 sides of the TPC provide further discriminating power against backgrounds of cosmogenic origin.

A total of 477.60±0.01 live days of data were collected between September 22, 2011 and September 1, 2013. For the results discussed below [9 10 11], this same data set ("low-background data") and the same set of event selection criteria were applied. Events consistent with noise, coincident with the muon veto, with more than one scintillation signal, or within 1 s of other events in the TPC were removed.

The same fiducial volume, defined as hexagonal with an apothem of 162 mm, was used for all the analyses. Only regions within this hexagonal volume that are >10 mm from the cathode and anode wire planes were included. This geometry corresponds to a ^{136}Xe mass of 76.5 kg, or 3.39×10^{26} atoms of ^{136}Xe. The total exposure is 100 kg·yr (736 mol·yr). In all of the analyses, an energy range (summed over all charge clusters in an event) of 980−9800 keV was used, to ensure that all of the charge clusters have near 100% efficiency of being reconstructed in three dimensions. Finally, only events that have fully reconstructed U-, V-, and Z-positions were considered.

3 Data Analysis

The ability to discriminate between β-like and γ-like events due to their topology, mainly whether the event is single-site (SS) or multi-site (MS), is the main reason behind EXO-200's good sensitivity as a double beta decay detector. At the Q-value, there is a 3 to 1 rejection of γ backgrounds. Most β events are single site in nature, while γ events tend to leave multiple distinct charge clusters after Compton scattering.

A Geant4-based Monte Carlo (MC) simulation of the detector and shielding (described in detail in [3]) is used to model the detector response. Comparison of data and MC in source runs (source agreements) validates the simulations. From the MC simulations, probability density functions (PDFs) separated for SS and MS are created. Periodic calibrations using γ sources (primarily ^{228}Th but also ^{60}Co, ^{226}Ra, and ^{137}Cs) determines the energy scale and resolution from fitting the full shape of the energy spectra between the data and the MC simulation. Separate energy scale and resolutions were determined for SS and MS.

To get the physics results, a binned maximum-likelihood (ML) fit is performed simultaneously in SS and MS with the 2-dimensional PDFs in energy and another variable (Standoff Distance for most of the analysis, a machine learning generated "discriminator" for the excited analysis) and the low background data set to search for $0\nu\beta\beta$ and other physics. Systematic uncertainties are taken into consideration by applying Gaussian constraints on the fit parameters. Profile likelihood scans are next performed for each signal separately to get the count that corresponds to 90% confidence level (C.L.) to determine the corresponding limit on the half-life.

For the Majoron and the excited state results, unique normalization parameters are calculated. Toy MC data sets with a nonzero number of signal events are generated from PDFs that have been skewed by the relative differences between data (calibration source data or a background subtracted spectrum from the physics run to represent $2\nu\beta\beta$) and MC. These toy data sets are then fit to the standard, un-skewed PDFs, and the resulting difference between the fitted and simulated number of excited state events is determined. This fractional difference is accounted for as a systematic error that is an allowed constraint in the normalization term of the fit.

4 Results

4.1 $0\nu\beta\beta$

The main objective of the EXO-200 experiment is of course the search for $0\nu\beta\beta$. A blind analysis, where the ROI was not looked at until all of the background models have been verified, resulted in a best fit value of 9.9 $0\nu\beta\beta$ count, consistent with the null hypothesis at 1.2σ [9]. While the half-life sensitivity of $1.9 \cdot 10^{25}$ yr was achieved, a half-life limit of $1.1 \cdot 10^{25}$ yr at 90% C.L. was set. Figure 3 left shows the SS (top) and MS (bottom) energy fit results.

4.2 Majoron

Majoron modes with indices of 1, 2, 3, and 7 were searched for independently in separate fits without the inclusion of $0\nu\beta\beta$ [10]. The best fit results are shown in Figure 3 right. No Majoron was observed and the corresponding limits on the half-life are shown in Table 1.

4.3 $2\nu\beta\beta$ *decay to excited state*

The decay to the excited state study [11] is the first EXO-200 analysis to use a Machine Learning technique. Several different Machine Learning algorithms were considered with a variety of input variables. Ultimately, Boosted Decision Tree (BDT) was chosen with 6 variables - energy, multiplicity, standoff distance, and the minimal energy difference among all of the charge clusters and one of 760.5 keV, 8181.5 keV, and 1579 keV (the energies of the emitted γ's and the sum

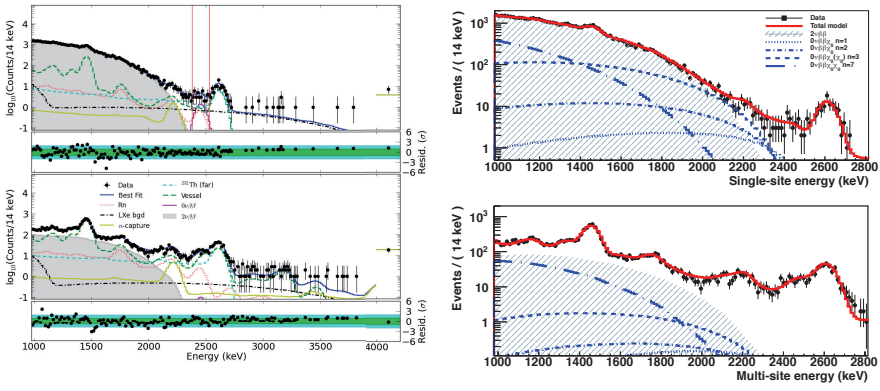

Figure 3 – The energy best fits for EXO-200 analysis. On the left, the SS (top) and MS (bottom) energy fit results for the $0\nu\beta\beta$ search are shown. The SS window marked by the red lines is the $0\nu\beta\beta$ region of interest (ROI). The SS (top) and MS (bottom) energy spectra of the various independent Majoron fits are shown on the right. The different blue dash lines represent different Majoron modes. For the Majoron searches, $0\nu\beta\beta$ was not a part of the fit.

Table 1: The half-life limits at the 90% C.L. for each Majoron modes searched by EXO-200.

Decay Mode	Spectral Index, n	$T_{1/2}$, yr
$0\nu\beta\beta\chi_0$	1	$> 1.2 \cdot 10^{24}$
$0\nu\beta\beta\chi_0$	2	$> 2.5 \cdot 10^{23}$
$0\nu\beta\beta\chi_0\chi_0$	3	$> 2.7 \cdot 10^{22}$
$0\nu\beta\beta\chi_0$	3	$> 2.7 \cdot 10^{22}$
$0\nu\beta\beta\chi_0\chi_0$	7	$> 6.1 \cdot 10^{21}$

of the two) - as the method with the best sensitivity and the minimal systematic uncertainties. The final fit was not conducted until after this choice of the machine learning algorithm.

A theoretical calculation, based on the $2\nu\beta\beta$ to ground state measured rate [3] and PSF [12] and NME [13] theoretical calculations, predicts a half-life of $\sim 10^{25}$ yr, with substantial uncertainty. Best fits by the EXO-200 search for the decay to the excited state are shown in Figures 4. A best fit value of 43 events was found with a 90% C.L. upper limit of 104 events. The resulting lower limit on the half-life of the $2\nu\beta\beta$ decay of ^{136}Xe to the first 0^+ excited state of ^{136}Ba is $T^{2\nu}_{1/2} > 6.9 \times 10^{23}$ yr at 90% C.L. This limit is slightly worse than the expected sensitivity of 1.7×10^{24} yr, see Figure 5 left. Like the Majoron results, the excited state fit was conducted without the inclusion of a search for $0\nu\beta\beta$.

5 Current Status of EXO-200 and progress toward nEXO

Unfortunately, EXO-200 was forced to take a nearly two year hiatus from February of 2014 to late January of 2016 due to an unforseen problem at the WIPP site in their radiation waste storage effort [14]. The EXO-200's remote recovery system worked successfully as designed, as the underground site power outage lasted a full year. Eventually after the power has been restored, the experimental recovery effort took about an year to get EXO-200 back to data taking. EXO-200 has now resumed the hardware electronic upgrades designed to lower the energy resolution. A deradonator has also been commissioned to improve the background in the region of interest.

While EXO-200 is planned to run for 3 additional years, the ultimate improvement in $0\nu\beta\beta$ sensitivity may be minimal. The more useful contribution for EXO-200 is to provide further

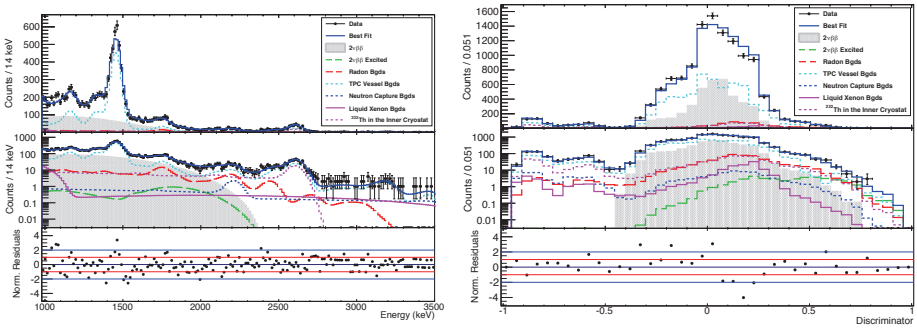

Figure 4 – The MS best fits from the excited decay search are shown. The left figure shows the energy fit. The right figure shows the fit of the "discriminator" variable. The excited state event distributions are given by the dashed green line (concentrating toward positive discriminator values). Data points are shown in black and residuals between data and the best fit are also shown for all non-zero bins.

knowledge and lessons toward the design of nEXO, the "next EXO" or the next phase with approximately 5 tonnes of liquid xenon. The current projected sensitivity for nEXO (assuming a lower energy resolution that may be attainable by EXO-200 after the current electronic upgrades) is good enough to fully probe the inverted mass hierarchy after five years or run time, see Figure 5 right. The nEXO design is hoping to benefit from additional improvements from self-shielding (the new design removes the cathode and its radioimpurities from the center of the detector), deeper location (it is currently designed with a move to SNOLAB in mind), and technological improvements of using silicon photomultipliers for scintillation detection and having a more efficient charge readout scheme for ionization detection. The projected nEXO sensitivity is 6.6×10^{27} yr.

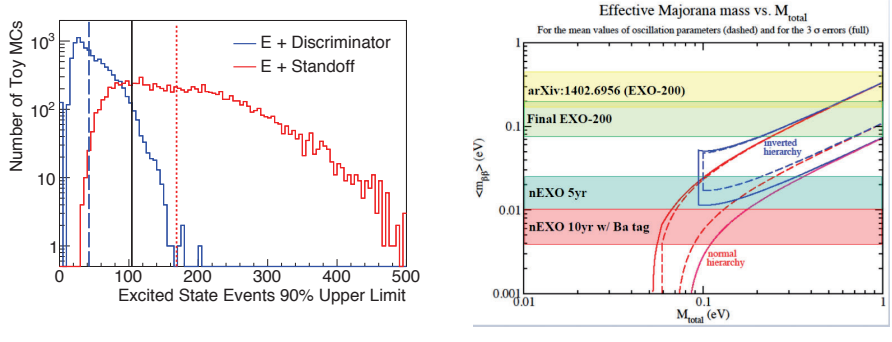

Figure 5 – Left: Distribution of 90% CL upper limits on the number of excited state events from toy MC data sets with no excited state events, using fits to energy and either standoff distance (red) or discriminator (blue). Median values are drawn with dashed lines, with the limit from data at 104 events drawn as a solid line. Right: The projected sensitivity to the effective neutrino mass (based on the expected sensitivity to $0\nu\beta\beta$ half-life) for the final EXO-200 result and the next phase nEXO, with and without Barium Tagging. nEXO with Barium Tagging could rule out the entire phase space for the inverted hierarchy of the neutrino mass.

Should the EXO barium tagging effort, the idea that the daughter ^{136}Ba ion can be positively identified from a candidate event in the $0\nu\beta\beta$ search energy window to eliminate nearly all backgrounds, proves to be successful. nEXO with barium tagging can completely cover the inverted hierarchy and probe into the normal hierarchy with a ten year runtime.

References

1. M. Goeppert-Mayer *Phys. Rev.* **48**, 512 (1935)
2. K.A. Olive *et al Chin. Phys.* **C38**, 090001 (2014)
3. J.B. Albert *et al* (EXO-200) *Phys. Rev.* C **81**, 015502 (2014)
4. A. S. Barabash *Phys. Rev.* C **81**, 035501 (2010)
5. A.A. Sonzogni *Nuclear Data Sheets* **95**, 837 (2002) data extracted from the ENSDF database, Oct. 9, 2015 `http://www.nndc.nbl.gov`
6. A. Dobi *et al Nucl. Instrum. Methods* A **620**, 594-598 (2010)
7. A. Dobi *et al Nucl. Instrum. Methods* A **675**, 40-46 (2012)
8. M. Auger *et al* (EXO-200) *JINST* **7**, P05010 (2012)
9. J.B. Albert *et al* (EXO-200) *Nature* **510**, 229 (2014)
10. J.B. Albert *et al* (EXO-200) *Phys. Rev.* D **90**, 092004 (2014)
11. J.B. Albert *et al* (EXO-200) *Phys. Rev.* C **93**, 035001 (2016)
12. J. Kotila and F. Iachello *Phys. Rev.* C **85**, 034316 (2012)
13. J. Barea, J. Kotila, and F.Iachello *Phys. Rev.* C **91**, 034304 (2015)
14. J. Vincent *The Verge* published March 27, 2015 at `http://www.theverge.com/2015/3/27/8299325/kitty-litter-nuclear-waste-accident-wipp`